Regulatory Toxicology and Pharmacology 70 (2014) 312–324

Contents lists available at ScienceDirect

Regulatory Toxicology and Pharmacology

journal homepage: www.elsevier.com/locate/yrtph

The acute effects of daily nicotine intake on heart rate – A toxicokinetic and toxicodynamic modelling study

M. Gajewska [a,b,d,*], A. Worth [a], C. Urani [b], H. Briesen [c], K.-W. Schramm [d,e]

[a] Systems Toxicology Unit and EURL ECVAM, Institute for Health and Consumer Protection, European Commission, Joint Research Centre, 21027 Ispra, VA, Italy
[b] University of Milano Bicocca, Dep. of Earth and Environmental Sciences, Piazza della Scienza 1, Milano, Italy
[c] TUM, Wissenschaftszentrum Weihenstephan für Ernährung und Landnutzung, Lehrstuhl für Systemverfahrenstechnik, Weihenstephaner Steig 23, 85350 Freising, Germany
[d] TUM, Wissenschaftszentrum Weihenstephan für Ernährung und Landnutzung, Department für Biowissenschaften, Weihenstephaner Steig 23, 85350 Freising, Germany
[e] Helmholtz Zentrum München – German Research Center for Environmental Health (GmbH), Molecular EXposomics (MEX), Ingolstädter Landstr.1, D-85764 Neuherberg, Germany

ARTICLE INFO

Article history:
Received 28 May 2014
Available online 24 July 2014

Keywords:
Physiologically-based toxicokinetic (PBTK) modelling
Physiologically-based toxicodynamic (PBTD) modelling
Nicotine

ABSTRACT

Joint physiologically-based toxicokinetic and toxicodynamic (PBTK/TD) modelling was applied to simulate concentration–time profiles of nicotine, a well-known stimulant, in the human body following single and repeated dosing. Both kinetic and dynamic models were first calibrated by using *in vivo* literature data for the Caucasian population. The models were then used to estimate the blood and liver concentrations of nicotine in terms of the Area Under Curve (AUC) and the peak concentration (C_{max}) for selected exposure scenarios based on inhalation (cigarette smoking), oral intake (nicotine lozenges) and dermal absorption (nicotine patches). The model simulations indicated that whereas frequent cigarette smoking gives rise to high AUC and C_{max} in blood, the use of nicotine-rich dermal patches leads to high AUC and C_{max} in the liver. Venous blood concentrations were used to estimate one of the most common acute effects, mean heart rate, both at rest and during exercise. These estimations showed that cigarette smoking causes a high peak heart rate, whereas dermal absorption causes a high mean heart rate over 48 h. This study illustrates the potential of using PBTK/TD modelling in the safety assessment of nicotine-containing products.

1. Introduction

Nicotine, a commonly used stimulant, has been investigated extensively in previous years, both in terms of *in vivo* and *in vitro* effects on human body. This psychoactive substance is known to increase heart rate, affect the nervous system and influence other biological processes including behavioural effects and metabolic responses (Fattinger et al., 1997; Perkins, 1992). Nicotine is an addictive drug and its consistent use is likely to result in the development of tolerance to (and dependence on) its actions. Cigarette smoking, as a delivery mechanism, is inherently more likely to produce addiction due to the extremely rapid pulmonary absorption of nicotine, occurring at a rate similar to intravenous administration (de Landoni, 1991). There is therefore interest in the development of nicotine replacement therapies based on alternative exposure routes (e.g., coated tablets, chewing gum, nasal spray, inhalator, microtablets and transdermal patches). Cigarettes vary in their nicotine content: the tobacco from bidi cigarettes has on average 21.2 mg/g of nicotine compared to the tobacco from filtered and unfiltered commercial cigarettes containing 16.3 and 13.5 mg/g of nicotine, respectively (Malson et al., 2001). To estimate a daily nicotine consumption, Benowitz et al. (1982) reported that low-, and high- nicotine commercial cigarettes deliver (with Federal Trade Commission [FTC] smoking machine) 1.2, 0.4 and 2.5 mg of nicotine, respectively. Transdermal patches, on the other hand, normally deliver from 5 to 30 mg nicotine and are applied

Abbreviations: A_{org}, C_{org}, amount and concentration of a chemical in given organ/blood [mg], [mg/L]; PC_{org}, organ-to-blood partition coefficients; $f_{\_card}$, cardiac output [L/h]; f_{org}, blood flow rate through organ [L/h]; V_{org}, volume of organ/blood [L]; CLR, renal clearance [L/h]; *fra*, *frb*, *frc*, absorbed fractions that reach liver from stomach, small and large intestine; ka_{stm}, absorption rate from stomach; ka_{SI}, absorption rate from small intestine [L/h]; ka_{LI}, absorption rate from large intestine [L/h]; kel_{LI}, elimination rate from large intestine [L/h]; k_{max}, k_{min}, stomach emptying rates to small intestine; Diss, dissolution rate from a coated tablet [L/h]; D_{SC}, D_{VE}, diffusion coefficients in *stratum corneum* and viable epidermis [cm^2/h]; *k*, release of a chemical from a patch; PC_{SC}, *stratum corneum*/vehicle partition coefficient; PC_{SCVE}, *stratum corneum*/viable epidermis partition coefficient; L_{SC}, L_{VE}, *L*, thickness of *stratum corneum*, viable epidermis, skin [cm]; Area, area of exposed skin [cm^2]; RR, respiratory rate [1/h]; ALV, alveolar ventilation [L/h]; VAT, mucous layer of inhaled/exhaled air [L].

* Corresponding author at: Systems Toxicology Unit and EURL ECVAM, Institute for Health and Consumer Protection, European Commission, Joint Research Centre, 21027 Ispra, VA, Italy.
E-mail address: Monika.Gajewska@ec.europa.eu (M. Gajewska).

http://dx.doi.org/10.1016/j.yrtph.2014.07.015
0273-2300/

over 24 h (de Landoni, 1991). *In vivo* experiments showed that less than 100% of the nicotine absolute dose in a patch reaches systemic circulation. The amount of nicotine absorbed has been reported to be between 65% and 90% of the total dose (Bannon et al., 1989; Gupta et al., 1993). This absorption was found independent of a dose and the undelivered amount is believed to be lost either by evaporation or possible skin metabolism.

Papathanasiou et al. (2013) recently studied the effect of nicotine smoking on heart rate at rest and during exercise in 298 young adults. The authors concluded that smokers had significantly higher resting heart rate values than non-smokers but the reverse was observed during exercise. The maximal values achieved during exercise were around 191–193 [bpm] (smokers) and 198–199 [bpm] (non-smokers).

There are many literature studies and reviews describing in detail the absorption, distribution, metabolism and excretion (ADME) processes of nicotine (Benowitz, 1990; Hukkanen et al., 2005).

Nicotine is a water and lipid soluble drug which, in the free base form, is readily absorbed via respiratory tissues, skin, and the gastrointestinal (GI) tract. Plasma protein binding was reported to be only around 5% (Yamazaki and Kanaoka, 2004). Nicotine readily reaches organs and tissues and undergoes extensive metabolism mainly in the liver by cytochrome P450 enzymes (mostly CYP2A6, and also by CYP2B6). A major metabolite of nicotine is cotinine (ca. 80% of nicotine conversion). Other metabolites include nicotine *N′*-oxide, nornicotine, nicotine isomethonium ion, 2-hydroxynicotine and nicotine glucuronide. Renal clearance accounts for up to 35% of total nicotine clearance (Tutka et al., 2005). Additionally, there are observed differences in plasma concentrations between smokers and nonsmokers suggesting differences in total clearance rates, with non-smokers showing faster clearance than smokers (Tutka et al., 2005; Yun et al., 2008). The apparent volume of distribution of nicotine was determined in one clinical study to be 2.0 L/kg in smokers and 3.0 L/kg in nonsmokers (Ellenhorn, 1988).

Due to rich literature resources and experimental data availability nicotine is a good candidate for further elaboration of joint Physiologically-based Toxicokinetic/Pharmacokinetic (PBTK/PBPK) and Toxicodynamic/Pharmacodynamic (PBTD/PBPD) models. Moreover, nicotine has a rapid onset of action therefore it can be used to model observable acute effects. Toxicodynamics is however a highly complex process and sensitive to the development of a physiological tolerance with respect to stimulant dose–response relationships. The theoretical framework should consequently be able to account for such "force-driving" tolerance and thereby reduce the effect of the drug (for instance, via incorporation of a "tolerance" compartment representing a hypothetical noncompetitive antagonist receptor, as described below). Various PBTK–TD models for nicotine are reported in the literature (Green et al., 1999; Porchet et al., 1988; Robinson et al., 1992; Teeguarden et al., 2013) and all present relatively simple but nevertheless satisfactory representations of the nicotine ADME process following the inhalation, dermal, and oral exposure routes.

The aim of this study was to apply a refined PBTK model (with the addition of sub-compartments in skin and GI tract and modification for drug effects) with respect to models previously developed in the scientific literature to simulate selected daily exposure scenarios of nicotine (both in terms of cigarette smoking and nicotine replacement therapy). The internal blood and liver concentrations are defined by the Area Under Curve (AUC) and the peak concentration (C_{max}) and are linked to the TD model which estimates one of the common acute effects, heart rate (mean and its trend in time), both at rest and during cycling exercise. This study builds on previous work by further applying PBTK/TD modelling to analyse nicotine ADME profiles resulting from various exposure conditions based on both single and repeated dosing.

2. Materials and methods

2.1. Experimental data used to calibrate and validate the PBTK model

For the purpose of this study we used the most complete *in vivo* dataset we could find in the public literature for the Caucasian population. For calibration of liver metabolism rates of nicotine to cotinine intravenous experimental data were used (Porchet et al., 1988). In this study, eight healthy subjects (all habitual smokers), in a state of rest, were given two intravenous (i.v.) administrations of nicotine (2.5 μg of nicotine per kg body weight (BW) per min for 30 min) at intervals of 1, 2 and 3.5 h. For validation, blood data of nine subjects after i.v. injection of nicotine (ca. 0.7 μg/kg BW per min for 180 min) were chosen (Fattinger et al., 1997).

For calibration of the oral PBTK model, single and repeated doses (once every 1.5 h for 12 h) of nicotine (4, 8, 12 mg) were ingested orally via a drinking straw (containing loose nicotine bitartrate particles) in a group of 24 smokers (D'Orlando and Fox, 2004). Mean plasma concentrations were calculated from individual nicotine levels presented in the paper. For validation purposes, nicotine-containing capsules coated with a polyacrylic carbomer, Carbopol 974P, (6 and 15 mg) were administered as a single dose to 12 subjects, all non-smokers (Green et al., 1999). Mean experimental serum nicotine concentrations were used from this study.

For calibration of the dermal PBTK model, nicotine patches (Nicolan™) were applied in various doses (15, 30 and 60 mg) directly to the skin of healthy human volunteers (all smokers) for 24 h as single doses and 30 mg applied in repetitive way once every 24 h for 7 days (Bannon et al., 1989). Mean measured plasma nicotine concentrations were published. For validation purposes, single and multiple applications of a nicotine transdermal system (NTS) were investigated on 13 healthy adult male smokers (1.5 mg/h of nicotine released over 24 h) (Gupta et al., 1993). Mean experimental plasma nicotine concentrations were presented.

For calibration of the inhalation PBTK model, cigarettes delivering nicotine doses of 0.4, 1.2, 2.5 mg were smoked (30 per day, with FTC smoking machine) by 12 healthy volunteers (all smokers) (Benowitz et al., 1982). Mean blood nicotine concentrations were measured. For validation, we used the inhalation of 0–64 mg/mL of nicotine by 24 healthy non-smoking subjects (Hansson et al., 1994).

2.2. Experimental data used to develop the PBTD model

The toxicodynamic model of heart rate was developed using data published by Porchet et al. (1988) and validated using experimental results of Fattinger et al. (1997). In both cases, heart rate responses to intravenous nicotine were measured at rest.

To simulate the effect of nicotine on heart rate during exercise, a literature study was chosen in which the effects of nicotine (transdermal 7 mg-nicotine patch) were measured on cycling endurance. The study was carried out on twelve healthy males who were non-smokers (Mündel and Jones, 2006).

2.3. Structure and parameters of the PBTK–TD models

2.3.1. PBTK model

The schematic representation of the PBTK model is shown in Fig. 1. The model consists of three compartments describing: (i) the inhalation process (inhaled and exhaled air linked to the lungs) (Kumagai and Matsunaga, 1995); (ii) the GI tract with 6 sub-compartments (for oral exposure only), Fig. 2; and (iii) the skin with the surface compartment and 4 skin sub-compartments (for dermal exposure only), Fig. 3. The sub-compartments serve to account for the complexity of the absorption process (especially the associated time-lag). Transport through all the organs, except for the skin layers is described by ordinary differential equations.

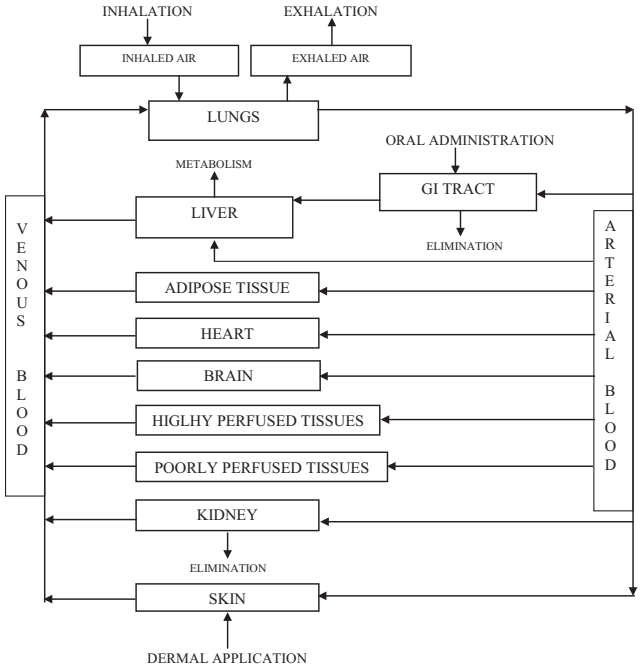

Fig. 1. General structure of the PBTK model.

In the GI tract, two different administration types are considered: administration via a straw and via dissolution from a coated tablet. A first-order rate of absorption from stomach, small and large intestine and stomach emptying rates are included according to Loizou and Spendiff (2004). Absorbed quantities are directed to the liver.

The skin is divided into *stratum corneum*, viable epidermis and dermis with blood mix. Uni-dimensional diffusion describes the transport in the skin according to Fick's second law with specified initial and boundary conditions (partial differential equations). The diffusion coefficient is different for *stratum corneum* and viable epidermis but assumed constant through the process of absorption.

The other organs/bio-fluids such as liver, kidney, adipose tissue, highly-perfused tissues, heart, brain, poorly-perfused tissues, and blood are single perfusion and accumulation sites in the model. Metabolism is assumed to occur only in the liver and excretion via urine and bile (to a lesser extent) is described by a first-order-rate constant. All the organs and blood are homogeneous with respect to the concentration of a chemical. Transport between blood and tissues is assumed to be flow-limited (transport barriers between free molecules of chemical in blood and tissue are negligible) and equilibrium between free and bound fractions in blood and tissue is instantaneous. It is further assumed that plasma accounts for 55% of blood volume and that the difference between blood and plasma levels is defined by a ratio coefficient. The model simulations for single and repeated dosing are carried out for the same ADME parameters.

The model equations are given in Appendix 1.

All physiological parameters for a reference man and woman are given in Table 1, after Brown and colleagues (Brown et al., 1997) and after (Kumagai and Matsunaga, 1995) for the respiratory parameters.

Optimization was performed for the most sensitive parameters (with respect to AUC in blood/plasma) identified by the Sensitivity Analysis according to Soetaert and Petzoldt (Soetaert and Petzoldt, 2010; Soetaert, 2010). These parameters were: nicotine metabolism rate to cotinine (V_{max}), nicotine dissolution from a tablet in the stomach (Diss), absorption from stomach (ka_{stm}) and small intestine (ka_{SI}), diffusion coefficient in *stratum corneum* (D_{SC}),

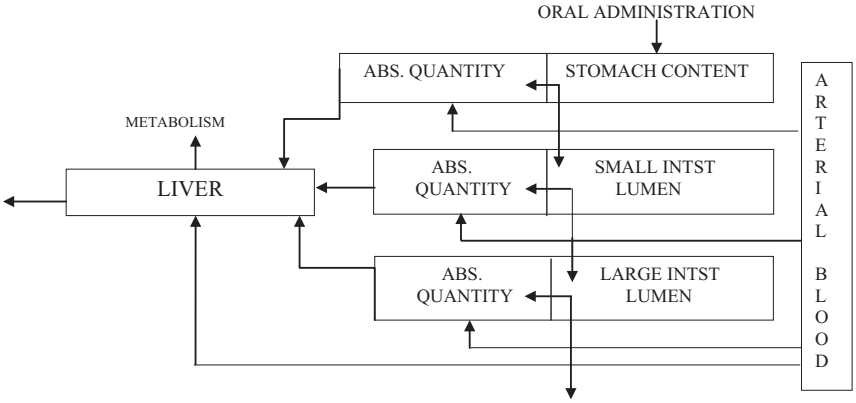

Fig. 2. GI tract divided into sub-compartments in PBTK model.

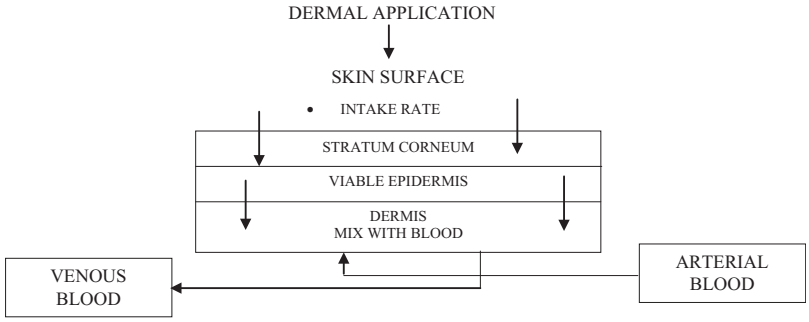

Fig. 3. Skin divided into sub-compartments in PBTK model.

Table 1
Physiological parameters for a reference woman and man.

Quantity	Reference woman	Reference man
Average body weight [kg]	60	75
Organ weights fractions (fractions of body weight)		
Liver	0.026	0.026
Adipose tissue	0.254	0.140
Lungs	0.0105	0.012
Kidney	0.0044	0.0044
Heart	0.0044	0.0044
Brain	0.02	0.02
GI tract	0.0265	0.025
Stomach	0.00337	0.00318
Small intestine	0.0146	0.0138
Large intestine	0.0085	0.0080
Poorly perfused tissues	0.36	0.42
Skin	0.08	0.108
Remaining organs/tissues	0.149	0.169
Blood	0.065	0.072
Venous blood	0.04875	0.054
Thickness of: skin, viable epidermis, *stratum corneum* [cm]	0.204, 0.0032, 0.0018	0.2906, 0.0047, 0.0017
Regional blood flow rates [fraction of cardiac output [L/h]		
Cardiac output [L/h]	$15 \cdot BW^{0.74}$	$15 \cdot BW^{0.74}$
Liver	0.25	0.24
Adipose tissue	0.055	0.04
Lungs	0.025	0.025
Kidney	0.19	0.2
Heart	0.04	0.04
Brain	0.114	0.144
Poorly perfused tissues	0.135	0.16
GI tract	0.14	0.13
Fractions of GI tract flow to stomach, small and large intestine	0.2, 0.6, 0.2	0.2, 0.6, 0.2
Skin	0.05	0.05
Remaining organs/tissues	0.001	0.001
Alveolar ventilation ALV [L/h]	288.549	326.8275
Respiratory rate RR [1/h]	840 (at rest) 1080 (at exercise)	840 (at rest) 1080 (at exercise)
Mucous layer or inhaled/exhaled air VAT [L]	0.1 (optimized)	0.2 (optimized)

nicotine release from patch (k), partition coefficient between patch and *stratum corneum* (PC_{SC}), nicotine water/air partition coefficient ($PC_{water,air}$).

Optimization was carried out by applying the Levenberg–Marquardt algorithm to nonlinear data fitting (Moré, 1978). The parameters were optimized always with respect to *in vivo* blood/plasma nicotine concentrations of smokers.

Diffusion and partition coefficients in viable epidermis were calculated by literature quantitative–structure activity relationships (QSARs) for skin permeation (median values were chosen): diffusion coefficient (Cleek and Bunge, 1993; Krüse et al., 2007; McCarley and Bunge, 2001; Yamaguchi et al., 2008) and *stratum corneum*/viable epidermis partition coefficient (Chinery and Gleason, 1993; McCarley and Bunge, 2001; Polak et al., 2012; Yamaguchi et al., 2008). The blood/air partition coefficient was also estimated using QSAR equations (Buist et al., 2012).

Tissue-to-blood partition coefficients for nicotine and cotinine were determined according to Schmitt (2008). The model calculates steady-state tissue: plasma partition coefficients based on the composition of the tissues in terms of water, neutral lipids, neutral and acidic phospholipids and proteins using the lipophilicity, the binding to phospholipid membranes, the pKa and the unbound fraction in blood plasma as compound specific parameters. For nicotine, calculations were done for pKa = 8, $LogP_{oct}$ = 1.17 (octanol–water partition coefficient) and fu = 0.95 (fraction unbound to proteins).

Metabolism of nicotine to cotinine in the liver is assumed to follow Michaelis–Menten kinetics. Metabolism to other substances in the liver follows first- order reaction rate with a rate constant- Kmet [L/h].

Table 2 provides the list of all the values of the PBTK model parameters.

2.3.2. PBTD model

The PBTD model is in accordance with the previously published nicotine-effect model (sigmoid E_{max} model) in which a "tolerance" compartment represents a hypothetical noncompetitive antagonist (Porchet et al., 1988) – Fig. 4. Use of this model in predicting toxicodynamics has already been explained in Holford and Sheiner (1981)). The modification in the model, introduced for a better fit and better description of pharmacological response curves, includes the addition of an exponent in the considered concentrations to modify the hyperbolic form of the original model (Eqs. (1) and (3)) (Davey et al., 1976).

In this work, we assume, in accordance with the model fitting results to available literature data, that this modification is necessary for the case of nicotine effects during exercise only. As in the paper of Porchet et al. (1988) to avoid identifiability problems, we additionally assume that the chemical concentration in blood (C_{ven}) is always much less than the concentration needed to produce half of the maximal effect ($C_{ven,50}$), i.e., $C_{ven} <<< C_{ven,50}$. Antagonist (tolerance) formation and elimination rates are assumed to constant (Eq. (2)) and are dependent on venous blood concentration of a stimulant. Since, however, it is only the unbound fraction of a drug in blood that causes an effect, the venous blood concentrations are corrected by the protein-binding coefficient (fu).

Modified sigmoid model with hypothetical noncompetitive antagonist (Porchet et al., 1988):

$$E = E_0 + \frac{\frac{E_{max}}{C^y_{ven,50}} \cdot C^y_{ven}}{\left(1 + \frac{C^y_{Ant}}{C^y_{Ant,50}}\right) \cdot \left(1 + \frac{C^y_{ven}}{C^y_{ven,50}}\right)} \approx E_0 + \frac{\frac{E_{max}}{C^y_{ven,50}} \cdot C^y_{ven}}{1 + \frac{C^y_{Ant}}{C^y_{Ant,50}}} \rightarrow E = E_0 + \frac{S \cdot C^y_{ven}}{1 + \frac{C^y_{Ant}}{C^y_{Ant,50}}} \quad (1)$$

Table 2
ADME parameters for nicotine.

Parameter	Value	References
Liver metabolism		
To cotinine: V_{max} [mg/h/BW]	28.1 nmol/mg of protein/h - > 319.785 mg/h- > 11.260 [mg/h/BW]; microsomal protein yield: 34–42 mg/g liver; (we took mean value) 38 mg/g liver	Optimized for (Fattinger et al., 1997; Porchet et al., 1988); Originally from Messina et al. (1997); scaled up according to Pelkonen and Turpeinen (2007)
To cotinine: Km [mg/L]	10.52 (mean 64.9 μM)	Messina et al. (1997)
To other metabolites: Kmet [L/h/BW]	0.1674	Teeguarden et al. (2013)
Renal clearance [L/h/BW]	0.036	Teeguarden et al. (2013)
Tissue-to-blood partition coefficients		
Liver	1.42	Schmitt (2008)
Poorly-perfused tissues	0.39	
Highly-perfused tissues	1.62	
Skin	0.38	
Brain	2.63	
Lungs	1.32	
Kidney	1.34	
GI tract	0.58	
Adipose tissue	0.19	
Oral model		
Dissolution from tablet Diss [1/h]	0.235	Optimized
Absorption rate from stomach ka_{stm} [1/h]	0.006	Optimized
ka_{SI} [1/h]	0.1 (tablet) 1 (straw)	Optimized
Stomach emptying rates: k_{max} [1/h]	8.16	Loizou and Spendiff (2004)
Stomach emptying rates: k_{min} [1/h]	0.005	Loizou and Spendiff (2004)
Absorption rate from large intestine ka_{LI} [1/h]	0.1	Optimized
Elimination rate from large intestine kel_{LI} [1/h]	0.1	Optimized
Dermal model		
Diffusion coefficient in *stratum corneum* D_{SC} [cm^2/h]	1.6×10^{-05}	Optimized
Diffusion coefficient in viable epidermis D_{VE} [cm^2/h]	9.6×10^{-05}	QSAR predicted (see text)
Release of nicotine from patch k [1/h]	0.06	optimized
Partition coefficient between patch and *stratum corneum* PC_{SC}	0.4	Optimized
Partition coefficient between *stratum corneum and* viable epidermis PC_{SCVE}	1.518	QSAR predicted (see text)
Blood-to-plasma concentration ratio RBP	1.2	ADMET predictor[a]
Inhalation model		
Blood/air partition coefficient log$PC_{blood,air}$	4.743	QSAR predicted (Buist et al., 2012)
Water/air partition coefficient $PC_{water,air}$	6000	Optimized

[a] http://www.simulations-plus.com/Products.aspx?pID=13.

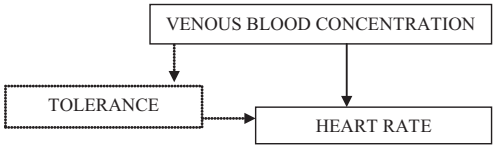

Fig. 4. Effect compartment – toxicodynamics.

$$V_{ven} \cdot \frac{dC_{Ant}}{dt} = k_{a,Ant} \cdot (fu \cdot C_{ven}) - k_{el,Ant} \cdot C_{Ant} \quad (2)$$

$$E = E_0 + \frac{S \cdot (fu \cdot C_{ven})^y}{1 + \left(\frac{C_{Ant}}{C_{Ant,50}}\right)^y} \quad (3)$$

Where:

E is the effect on heart rate,
E_0 is base-line effect,
E_{max} is the maximal effect,
C_{Ant} is the antagonist concentration [mg/L] (with respect to venous blood volume V_{ven}),
C_{ven} is the venous blood concentration of a chemical causing effect – a stimulant [mg/L],
$C_{ven,50}$ is the venous blood concentration of a chemical causing 50% of the maximal effect [mg/L],
$k_{a,Ant}$ and $k_{el,Ant}$ – are formation and elimination rates [L/h] of the antagonist,
fu – free fraction of a stimulant,
S – is equal to the ratio of E_{max} (maximal effect)/$(C_{ven,50})^y$ (concentration of a chemical causing half of the effect),
$C_{Ant,50}$ – the concentration of non-competitive antagonist (tolerance) attainable for a steady-state stimulant concentration,
y – exponent introduced as a deviation from the standard hyperbolic model.

The Sigmoid model parameters are listed in Table 3. Nicotine patch data were used to calibrate the exponent (y) for exercise conditions.

All the mathematical equations were programmed in R by combining functionalities of the following R packages: deSolve, ReacTran, PK and FME.[1] Ordinary differential equations (ODEs) were solved by the method *lsoda* available in the deSolve package, which switches automatically between stiff and non-stiff methods. The method of lines was used to solve PDEs.

[1] Available from The Comprehensive R Archive Network website: http://cran.r-project.org/ (last access: 16.12.2013).

Table 3
Toxicodynamic parameters for nicotine.

Parameter	Value	References
E_0 [bpm]	At rest: 61.2	Porchet et al. (1988)
	At rest: 64	Fattinger et al. (1997)
	During exercise: 145	Mündel and Jones (2006)
S [bpm/mg/L]	1000	Porchet et al. (1988)
$k_{a,Ant}$ [mg/L]	3	Optimized
$k_{el,Ant}$ [mg/L]	6	Optimized
$C_{50,Ant}$ [mg/L]	0.00772	Porchet et al. (1988)
y	1 (at rest)	
	0.6 (during exercise)	Optimized

2.4. Daily exposure design

Selected daily dosing conditions for nicotine together with web and literature references are presented in Table 4. They were selected for resting conditions and used unchanged for ongoing exercise to show the difference in heart rate changes at identical internal concentration levels. Only cigarette smoking was slightly modified by increasing the respiratory rate for the exercise condition. Daily dosing included the following consumption statistics:

(a) Smoked cigarettes per day of usual brand (1.2 mg over 4 min) (Benowitz et al., 1982):

- Occasional smokers – between 1 and 5 cigarettes per day (average 3 per day, one very 4 h)
- Light smokers – between 6 and 10 cigarettes per day (average 8 per day, one every 2 h)
- Regular smokers – between 11 and 20 cigarettes per day (assume 14 per day, one every 1 h)
- Heavy smokers – 21 or more cigarettes per day (assume 21 per day, one every 30 min)

(b) Nicotine patches:

- nicotine transdermal patch 7 mg applied once daily (Area = 22 cm^2)
- nicotine transdermal patch 14 mg applied once daily (Area = 22 cm^2)
- nicotine transdermal patch 21 mg applied once daily (Area = 22 cm^2)
- nicotine transdermal patch 42 mg (2 patches: 21 mg + 21 mg) applied once daily (Area = 2·22 cm^2 = 44 cm^2)

(c) nicotine lozenges – we assume dissolution rate from matrix calibrated according to (Green et al., 1999)

- 2-mg and 4 mg-nicotine applied lozenges every 1–2 h for 10 h. In this way, no more than 20 lozenges are used per day.

3. Results

3.1. Toxicokinetics of nicotine

3.1.1. Oral absorption

Simulated oral nicotine administration plasma data (via the Straw) used for the model calibration are shown in Fig. 5-left for single dose applications and Fig. 5-right for repeated dosing in accordance with experimental design specified in the reference source (D'Orlando and Fox, 2004). In this experiment it was noted that 8-times repeated administration of the highest dose of 12 mg did not show significant differences in plasma concentrations when compared to lower dosing of 8 mg. The authors explain that it is not clear whether it is due to limitations in the absorption of nicotine or simply variability in the patient population. The model simulations with assumed unchanged and constant parameters produced much higher results for the highest dose than the experimental values.

Oral absorption of nicotine in capsules (Green et al., 1999) with modelled dissolution from a coated matrix used for PBTK model validation is shown in Fig. 6. Only non-smokers participated in this experiment therefore the PBTK model simulations (with optimized parameters for smokers) clearly showed lower clearance than expected. Metabolism for nonsmokers would require ca. 1.2 times faster liver metabolism of nicotine provided there is no other elimination route. Renal clearance of nicotine was not among the most sensitive model parameters and increasing its value would not give

Table 4
Selected average daily exposure to nicotine.

Exposure route	Exposed amount	Number per day	References
Cigarettes	1.2 mg (usual brand) per 4 min	3,8,14,21	Benowitz et al. (1982), Fagerström (2005), National Tobacco Control Office (2002)
Dermal patch	7,14,21,42 mg per 24 h	1	emc (2014), Hamilton Health Sciences (2014)
Oral capsule nicotine lozenges	2, 4 mg	5, 10	MedlinePlus (2014)

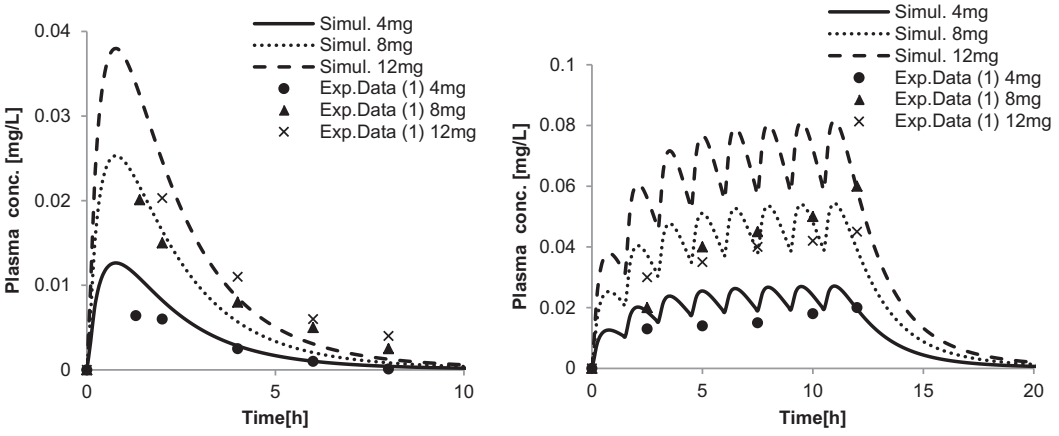

Fig. 5. Single (left) and repeated (right) oral absorption of nicotine using the Straw. Experimental data (1) taken from D'Orlando and Fox (2004).

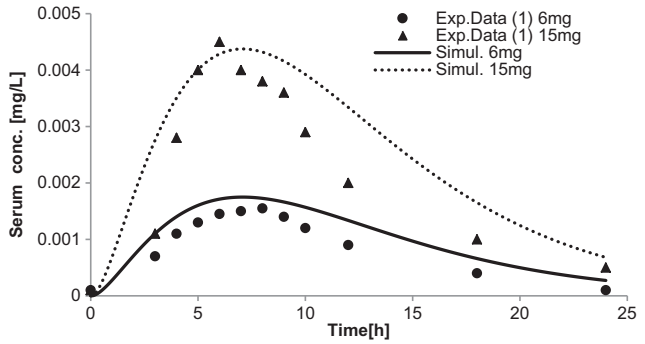

Fig. 6. Oral absorption of nicotine in capsules (single dose) in nonsmokers. Experimental data (1) taken from Green et al. (1999).

better presentation of nicotine concentration–time profile in serum of non-smokers.

3.1.2. Inhalation of nicotine

Fig. 7 shows blood concentrations of smokers after repeated smoking every 30 min for 4 min (doses = 0.4, 1.2 mg of nicotine) and for 3 min (dose = 2.5 mg of nicotine). We assumed that there was a constant inhaled nicotine concentration of absolute dose/0.05 [mg/L] and average smoking time of 4 min for low and regular doses, and 3 min for a high dose, to obtain better representation of experimental data. Moreover, we did not take into account metabolism of nicotine in the respiratory tract.

3.1.3. Dermal absorption of nicotine

Finally, dermal absorption of nicotine from patches is given in Fig. 8 (left) for single 24-h exposure and in Fig. 8 (right) for prolonged exposure (one nicotine patch per day up to 200 h) used in the calibration step (Bannon et al., 1989). In case of prolonged exposure, the model simulations were only slightly higher than the sampled experimental results. These experimental points were measured plasma concentrations prior to the application of a new nicotine patch (at the end of 24 h) – they are not peak concentrations resulting after a given application. That is why the model simulations, at first glance, appear ca. 4 times higher. There were small differences reported between measured plasma AUC of nicotine on day 1 and day 7 (Bannon et al., 1989) indicating no significant nicotine accumulation following chronic transdermal delivery. The model validation performed for a single application of 36 mg of nicotine in a patch (Gupta et al., 1993) is also shown in the Fig. 8 (left).

3.2. Toxicodynamics of nicotine

Sigmoid model predictions of increased heart rate are presented in Fig. 9 (left) for nicotine i.v. injections twice every 1, 2 and 3.5 h (at rest). Fig. 9 (right) shows the effect of nicotine patch on heart rate throughout the cycling exercise. The toxicodynamic parameters calibrated for intravenous nicotine injection at rest, that include tolerance formation and elimination, the ratio of E_{max} (maximal effect)/$(C_{ven,50})^{\gamma}$ and $C_{Ant,50}$ (but with a different base-line effect recorded in this experiment (Damirchi et al., 2009)) gave good

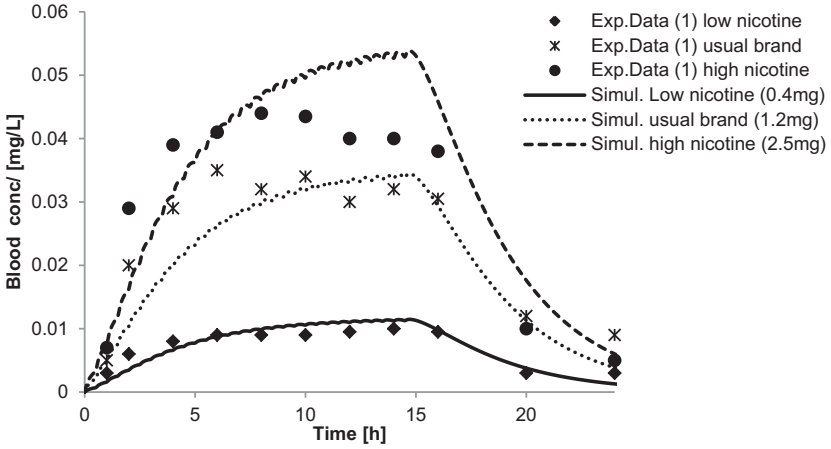

Fig. 7. Inhalation of nicotine via repeated smoking in smokers. Experimental data (1) taken from Benowitz et al. (1982).

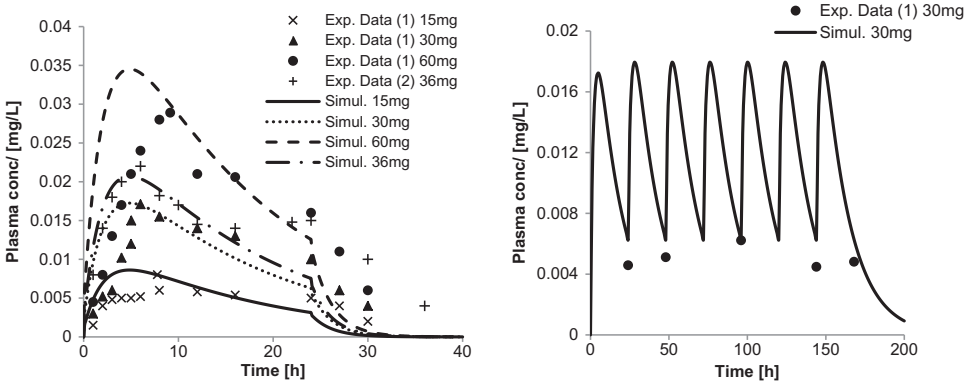

Fig. 8. Simulated concentration–time profiles in plasma for single (left) and repeated (right) applications of nicotine patches in smokers. Experimental data (1) are taken from Bannon et al. (1989) and (2) from (Gupta et al., 1993).

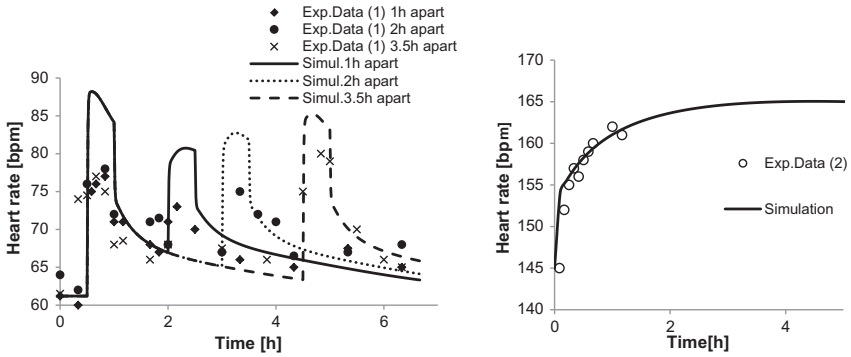

Fig. 9. Heart rate after double infusion of nicotine (left, at rest) and single dermal administration of nicotine patch (right, at exercise). Experimental data (1) taken from Porchet et al. (1988) and (2) from Mündel and Jones (2006).

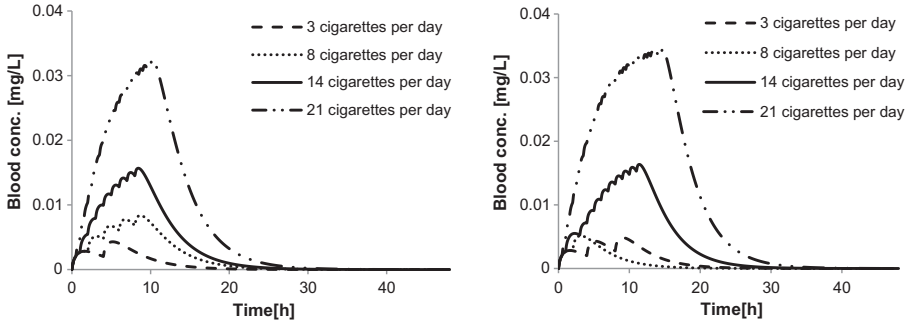

Fig. 10. Simulated blood concentrations of nicotine for selected daily repeated exposure to cigarettes (1.2 mg over 4 min) –at rest (left), during exercise (right).

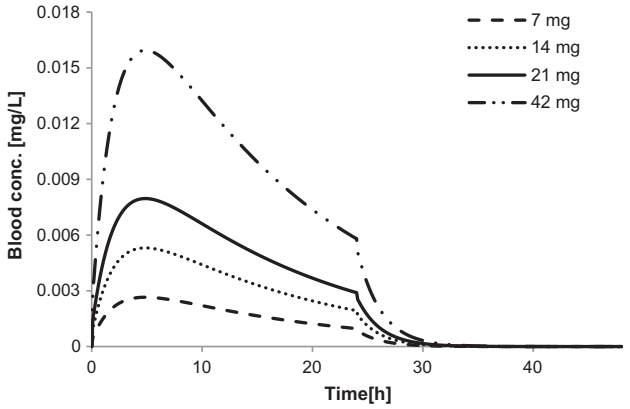

Fig. 11. Simulated blood concentrations of nicotine for selected daily single exposure to nicotine patch.

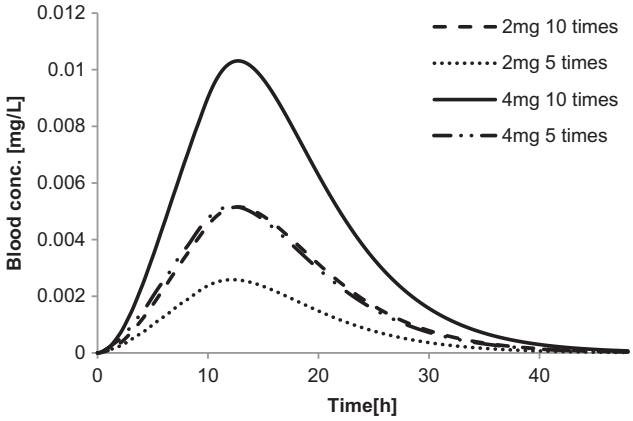

Fig. 12. Simulated blood concentrations of nicotine for selected repeated exposure within 24 h to nicotine lozenges.

predictive performance also in case of dermal absorption during exercise but an exponent smaller than 1 was necessary to obtain good fitting of experimental data. However, the need for this exponent may arise from the influence of exercise intensity on heart rate, smoker–nonsmoker differences in acute responses to nicotine (since nonsmokers data were used to calibrate the PBTD model during exercise; Mündel and Jones, 2006) or the combined effect of these factors. Additional experiments would be necessary to explore these factors.

3.3. Application of PBTK/TD models to simulate concentration–time profiles in blood and the effects of nicotine on heart rate following daily exposure profiles

In all the daily simulations of nicotine, we used a base-line heart rate of 61.2 [bpm] (Porchet et al., 1988) at rest and 145 [bpm] during exercise (Mündel and Jones, 2006).

Concentration–time profiles simulated for the daily exposure scenarios for cigarette smoking, nicotine patches and nicotine lozenges are shown in Figs. 10–12, whereas the simulated effects on heart rate are given in Figs. 13–15. Table 5 shows calculated AUC and peak concentrations for each exposure profile in the blood and liver. Cigarette smoking was simulated for different respiratory rates at rest and during exercise (see Table 1). This is why there are different blood concentrations in this case when compared to other exposure routes – increasing respiratory rate from 840 [1/h] to 1080 [1/h] produces ca. 1.5 times higher AUC and only slightly higher C_{max} values when compared to resting conditions. Table 6 provides estimates of mean heart rates over the duration of experiment (up to 48 h) for all four exposure routes.

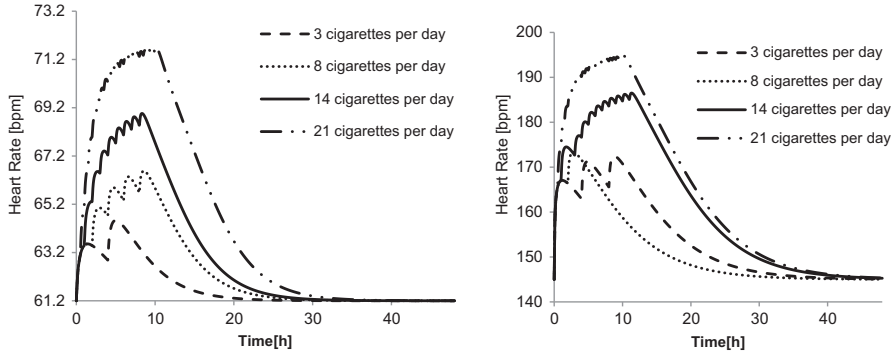

Fig. 13. Simulated mean heart rate following cigarette smoking at rest (left) and during exercise (right).

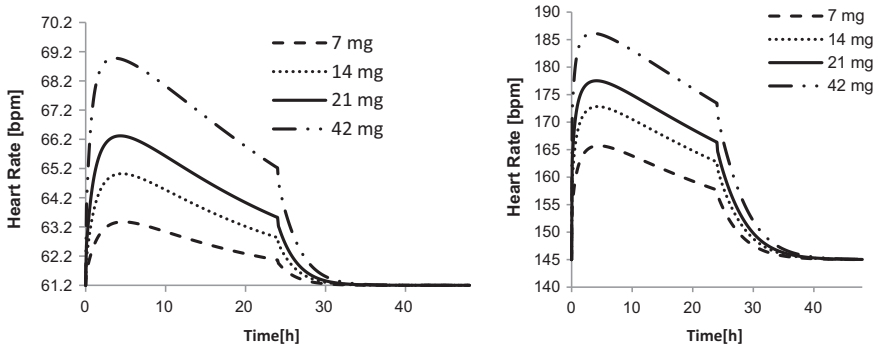

Fig. 14. Simulated mean heart rate following application of nicotine patches at rest (left) and during exercise (right).

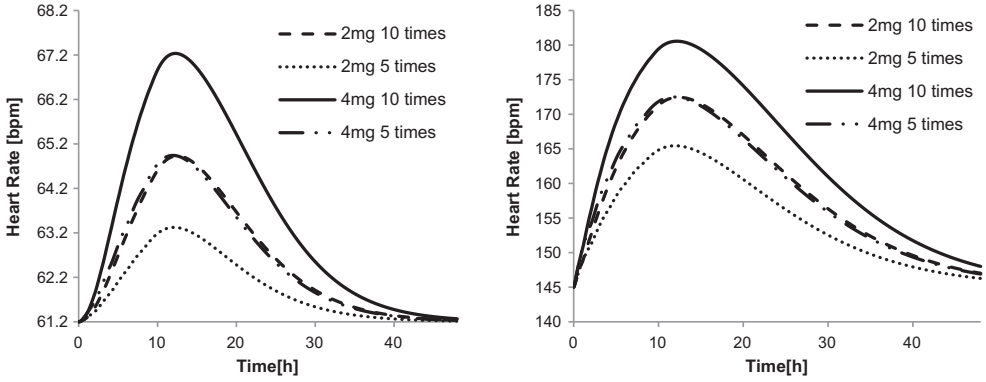

Fig. 15. Simulated mean heart rate following application of nicotine lozenges at rest (left) and during exercise (right).

4. Discussion

Simulating the toxicokinetic and dynamic behaviour of nicotine is complex even when the investigations are limited to the Caucasian population. The first modelling difficulty arises in accounting for differences in nicotine kinetics with respect to gender (i.e., varying nicotine and cotinine clearance), smoker-nonsmoker status (i.e., clearance of nicotine, nicotine binding to tissues, expression of metabolizing enzymes) and type of smoking – cigar smokers, users of snuff and chewing tobacco (i.e., rate of rise of nicotine) (Hukkanen et al., 2005). This, apart from pharmacodynamic issues, results in differences in blood/plasma concentrations (especially in the elimination phase) after single and prolonged exposure to nicotine.

When comparing predicted concentrations with experimental ones it is clear that the PBTK model performs best for exposure via the inhalation (cigarette smoking) and oral (with the straw) routes. Oral nicotine administration in carbomer capsules was also quite well represented by assuming a first-order rate of nicotine release from the tablet coating in the stomach. However, the model parameters calibrated previously for smokers did not produce a good match for the concentration–time profiles of nonsmokers. Absorption was simulated faster and elimination slower than observed (Green et al., 1999) – ca 1.2 times faster metabolism would produce better results. Experimental peak concentrations were achieved 7 h after nicotine dosing in the designed carbomer (Green et al., 1999) and 1–2 h after dosing with the straw (D'Orlando and Fox, 2004). Simulated peak levels were at 6.8 and 0.8 h, respectively indicating slightly faster calculated absorption than the observed one. Dermal exposure was the most difficult to model especially in the absorption phase. Experiments showed a peak concentration at 8 h (Bannon et al., 1989), whereas

Table 5
AUC and C_{max} values for all the exposures to nicotine.

Exposure route	AUC liver	AUC blood	C_{max} liver	C_{max} blood
Cigarettes (1.2 mg)				
3 per day	0.048 (rest)	0.035 (rest)	0.0061 (rest)	0.0043 (rest)
	0.072 (exercise)	0.053 (exercise)	0.0068 (exercise)	0.0048 (exercise)
8 per day	0.121 (rest)	0.0875 (rest)	0.012 (rest)	0.0084 (rest)
	0.0482 (exercise)	0.035 (exercise)	0.0073 (exercise)	0.0051 (exercise)
14 per day	0.217 (rest)	0.158 (rest)	0.0219 (rest)	0.0157 (rest)
	0.265 (exercise)	0.193 (exercise)	0.023 (exercise)	0.016 (exercise)
21 per day	0.507 (rest)	0.368 (rest)	0.0452 (rest)	0.0324 (rest)
	0.724 (exercise)	0.526 (exercise)	0.0478 (exercise)	0.0325 (exercise)
Dermal patches				
7 mg	0.159	0.046	0.009	0.003
14 mg	0.318	0.091	0.018	0.005
21 mg	0.477	0.137	0.028	0.008
42 mg	0.956	0.274	0.056	0.016
Nicotine lozenges				
2 mg (every 2 h)	0.102	0.043	0.0062	0.0026
2 mg (every 1 h)	0.204	0.086	0.0124	0.0051
4 mg (every 2 h)	0.204	0.086	0.0125	0.0052
4 mg (every 1 h)	0.409	0.172	0.0249	0.0103

Table 6
Predicted mean heart rates over simulation time for 4 administration routes.

Dose	Admin. route	Base-line heart rate (E_0) [bpm]	Mean heart rate at rest [bpm]	Mean heart rate during exercise [bpm]
2.5 μg/kg BW/min for 30 min 1 h apart	i.v	At rest = 61.2	69.206	–
2.5 μg/kg BW/min for 30 min 2 h apart	i.v	At rest = 61.2	69.558	–
2.5 μg/kg BW/min for 30 min 3.5 h apart	i.v	At rest = 61.2	69.196	–
0.7 μg/kg BW/min for 180 min	i.v	At rest = 64	71.350	–
Dermal patches				
7 mg		At rest = 61.2	62.008	154.508
14 mg	Dermal	during exercise	62.666	158.079
21 mg		=145	63.215	160.531
42 mg			64.436	165.256
Cigarettes (1.2 mg)				
3 per day		At rest = 61.2		
8 per day	Inhalation	during exercise	61.798	154.008
14 per day		=145	62.505	151.417
21 per day			63.215	161.235
			65.493	164.713
Nicotine lozenges				
2 mg (every 2 h)	Oral	at rest = 61.2	61.968	155.157
2 mg (every 1 h)		during exercise	62.606	159.138
4 mg (every 2 h)		=145	63.156	159.153
4 mg (every 1 h)			63.621	164.147

simulations indicated it at 4.9 h. One of the explanations could be that either the diffusion coefficient in skin or the rate of nicotine release are not constant over time or that there is a time delay in nicotine release from the patch. In fact, the measured *in vivo* release profiles of nicotine are not constant. They were found to be relatively linear for the first 8 h but then the absorption rate declined (Bannon et al., 1989). Experimental data for repeated smoking of low, average and high- nicotine brands of cigarettes resulted in nicotine concentrations in blood rising over the first 4–6 h after which they tended to plateau until smoking stopped (Benowitz et al., 1982). The PBTK model estimated an increase in blood levels up to the last cigarette (at 15 h) but this growth was ca. 5.3 times higher within the first 7 h. The major limitations of PBTK modelling in this study were in the underlying assumptions that: (i) there are no inter-individual and smoker–nonsmoker differences in the ADME model parameters; (ii) there is no nicotine in blood prior to exposure; and (iii) exposure is via only a single route; (iv) the model includes constant absorption parameters from the GI tract, respiratory tract and release from a patch and constant diffusion coefficient of nicotine through skin; (v) there is a need for using QSARs to predict partitioning between *stratum corneum* and viable epidermis as well as diffusion in epidermis due to lack of experimental data.

Application of the calibrated PBTK model to selected daily exposure scenarios showed that (Table 5):

- As expected, AUC and C_{max} in the blood were the highest after smoking 21 cigarettes per day (every 30 min) when compared to other exposure routes (AUC in blood was ca. 34% higher than that of 42 mg patch at rest and 92% higher with faster respiratory rate; C_{max} in blood was 103% (both at rest and during exercise) higher than after extreme dermal exposure).
- AUC and C_{max} in the liver were the highest for dermal application of two nicotine patches (42 mg) for 24 h over 44 cm^2 skin area (AUC in liver compared to that of smoking 21 cigarettes was found 89% (rest) and 32% (exercise) higher, whereas C_{max} in liver was 24% (rest) and 18% (exercise) higher).
- 2 mg of nicotine given orally every hour (10 times a day) is equivalent to 4 mg given orally every 2 h (5 times a day) in terms of AUC and C_{max}-based results.

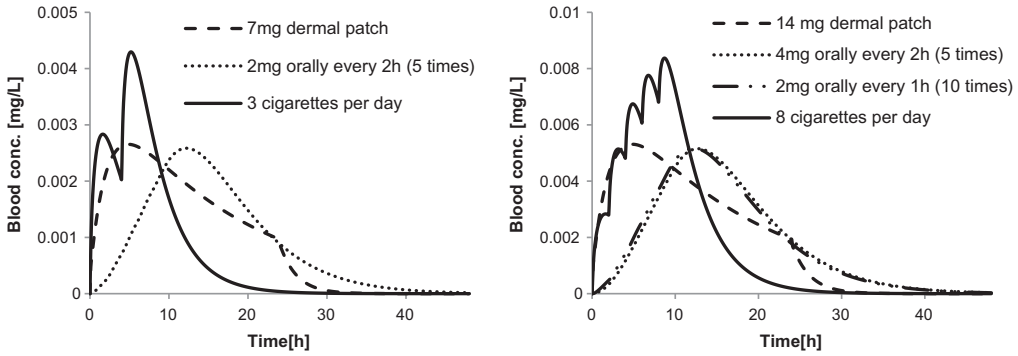

Fig. 16. Comparable exposure scenarios in terms of toxicokinetics – blood results.

- Assuming that the nicotine blood concentration, both in terms of AUC and C_{max}, is more relevant for systemic toxic effects, comparable exposure results were estimated for: 3 cigarettes per day ≈ 1 dermal patch 7 mg ≈ 2 mg of lozenges every 2 h (5 altogether); 8 cigarettes per day ≈ 14 mg dermal patch ≈ 4 mg of lozenges (5 altogether) or 2 mg lozenges (10 altogether) – Fig. 16.

Our choice of 4-min smoking time in these daily scenarios was based on the model calibrations with respect to *in vivo* data (Benowitz et al., 1982) and other literature studies such as the one of Mendelson et al. (2008)) in which the tested subjects smoked each cigarette for 4 min and took one 5 s- puff every 30 s. We assumed the same smoking duration for the exercise conditions and changed only the respiratory rate. By using a smoking time of 4 min we accounted for the worst-case scenario which is thus a conservative one in a safety assessment. In reality, there might be an increase in the puff frequency that makes a cigarette burn out faster; therefore a shorter time that 4 min could be more appropriate. To simulate a shorter smoking time would require, however, the availability of suitable data to verify the model performance in accurately estimating blood concentrations following smoking during exercise.

As shown in the results and indicated in the literature (Porchet et al. (1988)), the heart rate is well-described by a two-compartment PBTD model, but a modification (introduction of an exponent in relating the nicotine and antagonist concentrations to observable effect) might be necessary to obtain a better representation of heart rate increase during exercise conditions using the TD parameters calibrated for IV injection at rest (except for a base-line value). The need for this modification may arise from a variety of factors such as influence of exercise intensity, population effects, differences between smokers and non-smokers in terms of nicotine effects on heart rate, quality of experimental data, exposure route or combination of them.

TD model simulations indicate that the highest heart rate is achieved after heavy smoking of 21 cigarettes a day and equals 71.5 [bpm] (at rest, increase by 10.3 [bpm] from base effect) and 196 (during exercise, increase by 51[bpm] from the base effect). Our simulated heart rate values were in the range of experimental results published by Papathanasiou et al. for smokers during exercise: 191–193 bpm (Papathanasiou et al., 2013). At resting conditions our simulations indicated lower heart rates due to lower assumed base-line values than the ones of Papathanasiou et al. (61.2 vs. 72.8–76.4 bpm). When comparing mean heart rate estimates (Table 6) over up to 48 h we see, that it is dermal absorption that causes long-lasting higher heart rate. The reason behind it is probably pro-longed nicotine release from a patch and therefore a longer nicotine presence in the blood.

Whereas the application of PBTK–TD models in the simulation of selected daily exposure scenarios of nicotine has been usefully illustrated, further experiments are necessary to validate the modelling results and conclusions, especially given that environmental, genetic and other subject-specific differences are likely to affect human responses to nicotine. The approach illustrated here and the results obtained could nevertheless be used to guide the design of experiments that would help to assess the safety of nicotine-containing products. The applicability of PBTK modelling should be further investigated with respect to different exposure scenarios including consideration of other nicotine-containing products, the effects of other substances on nicotine ADME profiles, and combined (multi-route) exposure scenarios.

5. Conclusions

A joint PBTK–TD model for the Caucasian population, calibrated and validated by using various published nicotine blood/plasma concentrations (single and repeated dosing), has been applied to estimate and compare several daily exposure scenarios: cigarette smoking, oral and dermal absorption and their effects on acute increase in heart rate at rest and during exercise. Frequent cigarette smoking shows high AUC and C_{max} in the blood, and nicotine-rich dermal patches produce high AUC and C_{max} in the liver. The resulting toxicokinetics in blood after smoking of 3 cigarettes per day was found comparable to the use of a single 7 mg-dermal patch and 5 2 mg-lozenges every 2 h whereas smoking of 8 cigarettes per day was found comparable to a single use of 14-mg dermal patch or 10 2-mg lozenges every hour. However, the effects of smoking on heart rate are definitely higher than any of the investigated methods for nicotine therapy. Maximal heart rate while smoking was estimated to be ca. 1.35 times higher than the base-line value during a cycling exercise and ca. 1.17 times higher at rest. Multi-route exposure to nicotine was not investigated in this study and would require further experimentation and modelling.

Conflicts of interest

None.

Acknowledgments

This research was partially funded by the Seventh Framework Program (FP7/2007-2013) COSMOS (Integrated In Silico Models for the Prediction of Human Repeated Dose Toxicity of Cosmetics to Optimise Safety) Project and by Cosmetics Europe.

Appendix A.1

Adipose tissue (adp), highly perfused tissues – brain (brn), heart (hrt), poorly perfused tissues (ppt), remaining organs/tissues (ro), etc.:

$$\frac{dA_{org}}{dt} = f_{org} \cdot \left(C_{art} - \frac{C_{org}}{PC_{org}}\right);\ A_{org}(t=0) = 0;$$
$$C_{art} = \frac{C_{art}}{V_{art}};\quad C_{org} = \frac{A_{org}}{V_{org}} \tag{A1.1}$$

where: org = organ name (adp, hpt (brn, hrt), ppt, ro, etc.)

Kidney:

$$\frac{dA_{kid}}{dt} = f_{kid} \cdot \left(C_{art} - \frac{C_{kid}}{PC_{kid}}\right) - CLR \cdot \frac{C_{kid}}{PC_{kid}};\ A_{kid}(t=0) = 0;$$
$$C_{kid} = \frac{A_{kid}}{V_{kid}} \tag{A1.2}$$

Liver:

$$\frac{dA_{liv}}{dt} = Fl_{GIT} + FORM_{liv} + f_{liv} \cdot \left(C_{art} - \frac{C_{liv}}{PC_{liv}}\right) - MET_{liv};$$
$$A_{liv}(t=0) = 0;\quad C_{liv} = \frac{A_{liv}}{V_{liv}} \tag{A1.3}$$

For a parent compound:

$$\text{GI tract}: Fl_{GIT} = fra \cdot f_{git} \cdot \frac{C_{stm}}{PC_{git}} + frb \cdot f_{git} \cdot \frac{C_{SI}}{PC_{git}} + frc \cdot f_{git} \cdot \frac{C_{LI}}{PC_{git}}$$

$FORM_{liv} = 0$ (rate of formation of a given metabolite);

MET_{liv} – metabolism equations

Venous blood:

$$\frac{dA_{ven}}{dt} = f_{liv} \cdot \frac{C_{liv}}{PC_{liv}} + f_{hpt} \cdot \frac{C_{hpt}}{PC_{hpt}} + f_{ppt} \cdot \frac{C_{ppt}}{PC_{ppt}} + f_{ro} \cdot \frac{C_{ro}}{PC_{ro}} + f_{adp} \cdot \frac{C_{adp}}{PC_{adp}} + f_{kid} \cdot \frac{C_{kid}}{PC_{kid}} + Fl_{skn} - f_{\_crd} \cdot C_{ven};\quad A_{ven}(t=0) = 0;$$
$$C_{ven} = \frac{A_{ven}}{V_{ven}} \tag{A1.4}$$

$$\text{For dermal absorption}: Fl_{skn} = f_{skn} \cdot \frac{C_{skn}}{PC_{skn}}$$

Oral absorption:

Stomach content:

$$\frac{dA_{stm,cont}}{dt} = D_{rt} - ka_{stm} \cdot C_{stm,cont} - kGIT \cdot A_{stm,cont} \tag{A1.5}$$

$$\text{with}: C_{stm,cont} = \frac{A_{stm,cont}}{V_{stm}};\quad kGIT = \frac{k_{max}}{(1 + k_{min} \cdot C_{stm})}$$

and:

- admin. via gavage: $D_{rt} = 0;\ A_{stm,cont}(t=0) = \text{Dose}$
- admin. by a coated tablet: $D_{rt} = \frac{dA_{stm,cont,diss}}{dt} = -Diss \cdot A_{stm,cont,diss};\ A_{stm,cont,diss}(t=0) = \text{Dose}$

Stomach-absorbed quantity:

$$\frac{dA_{stm}}{dt} = ka_{stm} \cdot C_{stm,cont} + fra \cdot f_{git} \cdot \left(C_{art} - \frac{C_{stm}}{PC_{git}}\right);$$
$$A_{stm}(t=0) = 0;\quad C_{art} = \frac{A_{art}}{V_{art}};\quad C_{stm} = \frac{A_{stm}}{V_{stm}} \tag{A1.6}$$

Small Intestine lumen and absorbed quantity:

$$\frac{dA_{SI,lumen}}{dt} = kGIT \cdot A_{stm,cont} - (ka_{SI} + flow_{LI}) \cdot C_{SI,lumen};$$
$$A_{SI,lumen}(t=0) = 0;\quad C_{SI,lumen} = \frac{A_{SI,lumen}}{\left(\frac{3}{4} \cdot V_{int}\right)} \tag{A1.7}$$

$$\frac{dA_{SI}}{dt} = ka_{SI} \cdot C_{SI,lumen} + frb \cdot f_{git} \cdot \left(C_{art} - \frac{C_{SI,}}{PC_{git}}\right);$$
$$A_{SI}(t=0) = 0;\quad C_{SI} = \frac{A_{SI}}{\left(\frac{3}{4} \cdot V_{int}\right)} \tag{A1.8}$$

Large Intestine lumen and absorbed quantity:

$$\frac{dA_{LI,lumen}}{dt} = flow_{LI} \cdot C_{SI,lumen} - (kel_{LI} + ka_{LI}) \cdot C_{LI,lumen};$$
$$A_{LI,lumen}(t=0) = 0;\quad C_{LI,lumen} = \frac{A_{LI,lumen}}{\left(\frac{1}{4} \cdot V_{int}\right)} \tag{A1.9}$$

$$\frac{dA_{LI}}{dt} = ka_{LI} \cdot C_{LI,lumen} + frc \cdot f_{git} \cdot \left(C_{art} - \frac{C_{LI}}{PC_{git}}\right);$$
$$A_{LI}(t=0) = 0;\quad C_{LI} = \frac{A_{LI}}{\left(\frac{1}{4} \cdot V_{int}\right)} \tag{A1.10}$$

Skin absorption:

Skin surface:

$$(t < t_{appl})\ \text{AbsRate} = -k \cdot C_{form};\ (t \geq t_{appl})\ \text{AbsRate} = 0 \tag{A1.11}$$

Where: t_{appl} is the application time of a patch on the skin.

Stratum Corneum (SC):

$$\frac{dC_{SC,i}}{dt} \approx -\frac{q_{SC,i+1} - 2 \cdot q_{SC,i} + q_{SC,i-1}}{\left(\frac{Lsc}{N}\right)};\ i = 1 : NC_{SC,i} = \frac{A_{SC,i}}{V_{SC_i}} \tag{A1.12}$$

where: $q_{SC,i} = -D_{SC_i} \cdot \frac{C_{SC,i+1} - 2 \cdot C_{SC,i} + C_{SC,i-1}}{\left(\frac{Lsc}{N}\right)};\ i = 1 : N$

Initial and boundary conditions:

$$C_{SC}(t=0)|_{0 \leqslant x \leqslant L_{SC}} = 0$$
$$\frac{dC_{SC}}{dt}(t>0)|_{x=0} = k \cdot C_{form}$$
$$D_{SC} \cdot \frac{dC_{SC}}{dx}(t > t_{appl})|_{x=0} = 0$$
$$C_{SC}(t>0)|_{x=0} = PC_{SC} \cdot C_{form}$$
$$C_{SC}(t>0)|_{x=L_{SC}} = PC_{SCVE} \cdot C_{VE}$$

Viable Epidermis (VE):

$$\frac{dC_{VE,j}}{dt} \approx -\frac{q_{VE,j+1} - 2 \cdot q_{VE,j} + q_{VE,j-1}}{\left(\frac{Lve}{M}\right)};\ j = 1 : M \quad C_{VE,j} = \frac{A_{VE,j}}{V_{VE,j}} \tag{A1.13}$$

where: $q_{VE,j} = -D_{VE,j} \cdot \frac{C_{VE,j+1} - 2 \cdot C_{VE,j} + C_{VE,j-1}}{\left(\frac{L_{VE}}{M}\right)};\ j = 1 : M$

Initial and boundary conditions:

$$C_{VE}(t=0)|_{0 \leqslant y \leqslant L_{VE}} = 0$$
$$C_{VE}(t>0)|_{y=0} = \frac{C_{SC,i=N}}{PC_{SCVE}}$$
$$D_{SC} \frac{dC_{SC}}{dx}|_{x=L_{SC}} = D_{VE} \cdot \frac{dC_{VE}}{dy}|_{y=0}$$
$$C_{VE}(t>0)|_{y=L_{VE}} = PC_{skn} \cdot C_{skn}$$

Dermis and mix with the blood:

$$\frac{dA_{skn}}{dt} = f_{skn} \cdot \left(C_{art} - \frac{C_{skn}}{PC_{skn}}\right) + q_{VE,j=M} \cdot \text{Area};\quad A_{skn}(t=0) = 0;$$
$$C_{skn} = \frac{A_{skn}}{10^{-3} \cdot Vde} \tag{A1.14}$$

Inhalation:

Inhaled air tract:

$$\frac{dA_{INH}}{dt} = ALV \cdot \frac{C_{exp}}{PC_{water,air}} + 2 \cdot RR \cdot C_{EXH} - ALV \cdot \frac{C_{INH}}{PC_{water,air}} - 2 \cdot RR \cdot C_{INH};$$

$$A_{INH}(t=0) = 0; \quad C_{INH} = \frac{A_{INH}}{VAT} \tag{A1.15}$$

Exhaled air:

$$\frac{dA_{EXH}}{dt} = ALV \cdot \frac{C_{lng}}{PC_{water,air}} + 2 \cdot RR \cdot C_{INH} - ALV \cdot \frac{C_{EXH}}{PC_{water,air}} - 2 \cdot RR \cdot C_{IEXH};$$

$$A_{EXH}(t=0) = 0; \quad C_{EXH} = \frac{A_{EXH}}{VAT} \tag{A1.16}$$

Lungs:

$$\frac{dA_{lng}}{dt} = f_{lng} \cdot \left(C_{ven} - PC_{blood,air} \cdot \frac{C_{lng}}{PC_{lng}}\right) + ALV \cdot \frac{C_{INH}}{PC_{water,air}} - \frac{ALV}{PC_{water,air}} \cdot \frac{C_{Ilng}}{PC_{lng}}; \quad A_{lng}(t=0) = 0; \quad C_{lng} = \frac{A_{lng}}{V_{lng}} \tag{A1.17}$$

Arterial blood:

$$\frac{dA_{art}}{dt} = f\_crd \cdot \left(\frac{C_{lng}}{PC_{lng}} - PC_{blood,air} \cdot C_{art}\right); \quad A_{art}(t=0) = 0 \tag{A1.18}$$

References

Bannon, Y.B., Corish, J., Corrigan, O.I., Devane, J.G., Kavanagh, M., Mulligan, S., 1989. Transdermal delivery of nicotine in normal human volunteers: a single dose and multiple dose study. Eur. J. Clin. Pharmacol. 37, 285–290.

Benowitz, N.L., 1990. Pharmacokinetic considerations in understanding nicotine dependence. Ciba Found. Symp. 152, 186–200, discussion 200.

Benowitz, N.L., Kuyt, F., Jacob III, P., 1982. Circadian blood nicotine concentrations during cigarette smoking. Clin. Pharmacol. Ther. 32, 758–764.

Brown, R.P., Delp, M.D., Lindstedt, S.L., Rhomberg, L.R., Beliles, R.P., 1997. Physiological parameter values for physiologically based pharmacokinetic models. Toxicol. Ind. Health 13, 407–484.

Buist, H.E., Wit-Bos, L.D., Bouwman, T., Vaes, W.H.J., 2012. Predicting blood:air partition coefficients using basic physicochemical properties. Regul. Toxicol. Pharmacol. 62, 23–28.

Chinery, R.L., Gleason, A.K., 1993. A compartmental model for the prediction of breath concentration and absorbed dose of chloroform after exposure while showering. Risk Anal. 13, 51–62.

Cleek, R.L., Bunge, A.L., 1993. A new method for estimating dermal absorption from chemical exposure. 1. General approach. Pharm. Res. 10, 497–506.

D'Orlando, K.J., Fox, B.S., 2004. Tolerability and pharmacokinetics of single and repeated doses of nicotine with The Straw, a novel nicotine replacement product. Nicotine Tob. Res. 6, 63–70.

Damirchi, A., Rahmani-Nia, F., Mirzaie, B., Hasan-Nia, S., Ebrahimi, M., 2009. Effect of caffeine on metabolic and cardiovascular responses to submaximal exercise in lean and obese men. Biomed. Hum. Kinet. 1, 31–35.

Davey, A., Marriott, A., Stockham, M.A., 1976. Fitting a general sigmoid model to pharmacological response curves [proceedings]. Br. J. Pharmacol. 58, 289P–290P.

De Landoni, J.H., 1991. IPSC INCHEM: Nicotine [WWW Document]. URL <http://www.inchem.org/documents/pims/chemical/nicotine.htm>.

Ellenhorn, M., 1988. Diagnostics and Treatment of Human Poisoning, first ed. Elsevier Science Publishers, pp. 912–920.

emc, 2014. NiQuitin 21 mg Transdermal Patches [WWW Document]. URL <http://www.medicines.org.uk/emc/medicine/15340/SPC/NiQuitin+21+mg+transdermal+patches>.

Fagerström, K., 2005. The nicotine market: an attempt to estimate the nicotine intake from various sources and the total nicotine consumption in some countries. Nicotine Tob. Res. 7, 343–350.

Fattinger, K., Verotta, D., Benowitz, N.L., 1997. Pharmacodynamics of acute tolerance to multiple nicotinic effects in humans. J. Pharmacol. Exp. Ther. 281, 1238–1246.

Green, J.T., Evans, B.K., Rhodes, J., Thomas, G.A.O., Ranshaw, C., Feyerabend, C., Russell, M.A.H., 1999. An oral formulation of nicotine for release and absorption in the colon: its development and pharmacokinetics. Br. J. Clin. Pharmacol. 48, 485–493.

Gupta, S.K., Benowitz, N.L., Jacob III, P., Rolf, C.N., Gorsline, J., 1993. Bioavailability and adsorption kinetics of nicotine following application of a transdermal system. Br. J. Clin. Pharmacol. 36, 221–227.

Hamilton Health Sciences, 2014. Adult Nicotine Replacement Therapy (NRT) Order Set.

Hansson, L., Choudry, N.B., Karlsson, J.-A., Fuller, R.W., 1994. Inhaled nicotine in humans: effect on the respiratory and cardiovascular systems. J. Appl. Physiol. 76, 2420–2427.

Holford, N.H.G., Sheiner, L.B., 1981. Understanding the dose–effect relationship: clinical application of pharmacokinetic–pharmacodynamic models. Clin. Pharmacokinet. 6, 429–453.

Hukkanen, J., Jacob III, P., Benowitz, N.L., 2005. Metabolism and disposition kinetics of nicotine. Pharmacol. Rev. 57, 79–115.

Krüse, J., Golden, D., Wilkinson, S., Williams, F., Kezic, S., Corish, J., 2007. Analysis, interpretation, and extrapolation of dermal permeation data using diffusion-based mathematical models. J. Pharm. Sci. 96, 682–703.

Kumagai, S., Matsunaga, I., 1995. Physiologically based pharmacokinetic model for acetone. Occup. Environ. Med. 52, 344–352.

Loizou, G.D., Spendiff, M., 2004. A human PBPK model for ethanol describing inhibition of gastric motility. J. Mol. Histol. 35, 687–696.

Malson, J.L., Sims, K., Murty, R., Pickworth, W.B., 2001. Comparison of the nicotine content of tobacco used in bidis and conventional cigarettes. Tob. Control 10, 181–183.

McCarley, K.D., Bunge, A.L., 2001. Pharmacokinetic models of dermal absorption. J. Pharm. Sci. 90, 1699–1719.

MedlinePlus, 2014. Nicotine Lozenges [WWW Document]. URL <http://www.nlm.nih.gov/medlineplus/druginfo/meds/a606019.html>.

Mendelson, J.H., Goletiani, N., Sholar, M.B., Siegel, A.J., Mello, N.K., 2008. Effects of smoking successive low- and high-nicotine cigarettes on hypothalamic–pituitary–adrenal axis hormones and mood in men. Neuropsychopharmacology 33, 749–760.

Messina, E.S., Tyndale, R.F., Sellers, E.M., 1997. A major role for CYP2A6 in nicotine C-oxidation by human liver microsomes. J. Pharmacol. Exp. Ther. 282, 1608–1614.

Moré, J.J., 1978. The Levenberg–Marquardt algorithm: implementation and theory. Lect. Notes Math. 630, 105–116.

Mündel, T., Jones, D.A., 2006. Effect of transdermal nicotine administration on exercise endurance in men. Exp. Physiol. 91, 705–713.

National Tobacco Control Office, 2002. Promoting a Tobacco Free Society: Cigarette Smoking Trends [WWW Document]. URL <http://www.ntco.ie/research.asp>.

Papathanasiou, G., Georgakopoulos, D., Papageorgiou, E., Zerva, E., Michalis, L., Kalfakakou, V., Evangelou, A., 2013. Effects of smoking on heart rate at rest and during exercise, and on heart rate recovery, in young adults. Hellenic J. Cardiol. 54, 168–177.

Pelkonen, O., Turpeinen, M., 2007. In vitro–in vivo extrapolation of hepatic clearance: biological tools, scaling factors, model assumptions and correct concentrations. Xenobiotica 37, 1066–1089.

Perkins, K.A., 1992. Metabolic effects of cigarette smoking. J. Appl. Physiol. 72, 401–409.

Polak, S., Ghobadi, C., Mishra, H., Ahamadi, M., Patel, N., Jamei, M., Rostami-Hodjegan, A., 2012. Prediction of concentration–time profile and its inter-individual variability following the dermal drug absorption. J. Pharm. Sci. 101, 2584–2595.

Porchet, H.C., Benowitz, N.L., Sheiner, L.B., 1988. Pharmacodynamic model of tolerance: application to nicotine. J. Pharmacol. Exp. Ther. 244, 231–236.

Robinson, D.E., Balter, N.J., Schwartz, S.L., 1992. A physiologically based pharmacokinetic model for nicotine and cotinine in man. J. Pharmacokinet. Biopharm. 20, 591–609.

Schmitt, W., 2008. General approach for the calculation of tissue to plasma partition coefficients. Toxicol. In Vitro 22, 457–467.

Soetaert, K., 2010. R package FME: Inverse Modelling, Sensitivity, Monte Carlo – Applied to a Dynamic Simulation Model.

Soetaert, K., Petzoldt, T., 2010. Inverse modelling, sensitivity and Monte Carlo analysis in R using package FME. J. Stat. Softw. 33, 1–28.

Teeguarden, J.G., Housand, C.J., Smith, J.N., Hinderliter, P.M., Gunawan, R., Timchalk, C.A., 2013. A multi-route model of nicotine–cotinine pharmacokinetics, pharmacodynamics and brain nicotinic acetylcholine receptor binding in humans. Regul. Toxicol. Pharmacol. 65, 12–28.

Tutka, P., Mosiewicz, J., Wielosz, M., 2005. Pharmacokinetics and metabolism of nicotine. Pharmacol. Rep. 57, 143–153.

Yamaguchi, K., Mitsui, T., Aso, Y., Sugibayashi, K., 2008. Structure–permeability relationship analysis of the permeation barrier properties of the stratum corneum and viable epidermis/dermis of rat skin. J. Pharm. Sci. 97, 4391–4403.

Yamazaki, K., Kanaoka, M., 2004. Computational prediction of the plasma protein-binding percent of diverse pharmaceutical compounds. J. Pharm. Sci. 93, 1480–1494.

Yun, H.-Y., Seo, J.-W., Choi, J.-E., Baek, I.-H., Kang, W., Kwon, K.-I., 2008. Effects of smoking on the pharmacokinetics and pharmacodynamics of a nicotine patch. Biopharm. Drug Dispos. 29, 521–528.